

Improvement of electron beam quality in optical injection schemes using negative plasma density gradients

G. Fubiani,^{*} E. Esarey,[†] C. B. Schroeder, and W. P. Leemans[†]

Ernest Orlando Lawrence Berkeley National Laboratory, University of California, Berkeley, California 94720, USA

(Received 27 July 2005; published 6 February 2006)

Enhanced electron trapping using plasma density down-ramps as a method for improving the performance of laser injection schemes is proposed and analyzed. A decrease in density implies an increase in plasma wavelength, which can shift a relativistic electron from the defocusing to the focusing region of the accelerating wakefield, and a decrease in wake phase velocity, which lowers the trapping threshold. The specific method of two-pulse colliding pulse injector is examined in detail using a three-dimensional test particle tracking code. A density down-ramp with a change of density on the order of tens of percent over distances greater than the plasma wavelength leads to an enhancement of charge by two orders in magnitude or more, up to the limits imposed by beam loading. The accelerated bunches are ultrashort (fraction of the plasma wavelength—e.g., ~ 5 fs), high charge (>20 pC at modest injection laser intensity $\sim 10^{17}$ W/cm²), with a relative energy spread of a few percent at a mean energy of ~ 25 MeV, and a normalized root-mean-square emittance of the order of 0.5 mm mrad.

DOI: [10.1103/PhysRevE.73.026402](https://doi.org/10.1103/PhysRevE.73.026402)

PACS number(s): 52.38.Kd

I. INTRODUCTION

Compared to standard radio-frequency (rf) linear accelerators, advanced accelerators using plasmas can produce much higher acceleration gradients, in excess of 10 GeV/m, without the limitation of breakdown. In a plasma, the wavelength of the acceleration field is the plasma wavelength $\lambda_p = 2\pi c / \omega_p$ or $\lambda_p[\text{m}] \approx 3.3 \times 10^4 (n_0[\text{cm}^{-3}])^{-1/2}$, where n_0 is the plasma density, c is the speed of light, $\omega_p = (4\pi n_0 e^2 / m_e)^{1/2}$ is the plasma frequency, m_e is the electron mass, and $-e$ is the electron charge. For example, a laser wakefield accelerator (LWFA) [1] in the standard regime typically has a density of the order of $n_0 \approx 10^{18}$ cm⁻³ and a plasma wavelength of the order of $\lambda_p \approx 30$ μm . If a monoenergetic electron bunch is injected into a wakefield such that it is accelerated while maintaining a small energy spread, then it is necessary for the bunch to occupy a small fraction of the wake period, on the order of a few femtoseconds. This requires femtosecond accuracy in the injection process, which is problematic for current state-of-the-art photocathode radio-frequency electron guns.

Several injection mechanisms of plasma electrons into the accelerating wake have been described that rely on self-trapping. In a homogeneous plasma, self-trapping can occur by driving the wake to the wave-breaking limit in the self-modulated LWFA regime [2,3], in the highly nonlinear blow-out or bubble regime [4,5], or in the two-dimensional wave-breaking regime [6]. In an inhomogeneous plasma, a gradual density down-ramp will eventually lead to wave breaking some distance behind the drive beam, due to decrease in the wake phase velocity on the ramp [7,8]. Alternatively, a strong drive pulse can lead to trapping at a sudden discontinuity in the plasma density [9].

In an effort to improve the trapped bunch quality over single-beam methods, several injection methods have been proposed that utilize additional injection laser pulses. The motivation behind using additional injection pulses is to have more control over the injection process, provided the drive pulse does not create a wake of sufficient amplitude to self-trap background plasma electrons (so-called “dark-current free” powering of plasmas has recently been observed in a channel guided LWFA [10]). The injection pulse can be used to turn on and off the injection process; e.g., injection only occurs when the injection pulse intersects with the wake. The ponderomotive force associated with the envelope of a single injection laser pulse can be used to boost the electron momentum and phase such that they become trapped in the wakefield [11–13]. Typically, ponderomotive injection methods require high intensities $I > 10^{18}$ W/cm² (corresponding to a normalized laser strength $a \approx 8.6 \times 10^{-10} \lambda[\mu\text{m}] I^{1/2}[\text{W}/\text{cm}^2] > 1$) in both the pump and injection laser pulses.

Alternatively, the slow phase velocity beat wave (interference term) produced by the collision of two counterpropagating (or intersecting at an angle) lasers can be used in either a three-pulse [14,15] or two-pulse [16–19] configuration. In the original colliding pulse injector (CPI) concept, three short laser pulses were used for electron injection [14,15]. The pump pulse generates a plasma wake through its ponderomotive force, as in the standard LWFA. The two injection lasers—one pulse propagating in the forward direction behind the pump laser pulse and the other in the backward direction—collide at a predetermined phase of the plasma wake. During this collision, the beating of the injection laser pulses generates a beat wave with a slow phase velocity that kicks a subset of the background plasma electrons which can be trapped and accelerated. A simplified CPI configuration was proposed and analyzed by Fubiani and co-workers [16,17,19] that uses only two laser pulses with parallel polarizations: an intense pump pulse for wakefield generation and a single counterpropagating (or propagating at a

^{*}Also at the University of Paris XI (Orsay), France.

[†]Also at the University of Nevada, Reno.

finite angle) injection pulse. Injection is the result of the laser beat wave produced when the backward injection pulse collides with the trailing portion of the pump pulse. This configuration has the advantages of being easier to implement in comparison to the three-pulse CPI scheme and of requiring less intensity in the injection pulse compared to the ponderomotive injection scheme, since injection is the result of the laser beat wave as opposed to the ponderomotive force of a single injection pulse.

In this paper, a negative plasma density gradient is proposed and analyzed as a method for enhancing the electron beam quality in laser injection schemes. If a laser injection scheme is operated close to threshold, electrons will be injected into the region of the wake that is accelerating but defocusing. To have a trapped electron bunch that is both accelerated and focused, it is necessary to shift the bunch forward in phase. This can be accomplished with a downward density ramp. As the density decreases, the plasma wavelength increases; thus, a relativistic electron will be shifted forward in phase relative to the wake. This can shift an electron from the defocusing to the focusing region of the accelerating wake. In addition, if injection occurs on the density down-ramp, the trapping can occur more readily since the phase velocity of the wake is lowered on the down-ramp. Numerical examples are given based on a three-dimensional (3D) particle tracking code for the specific case of the two-pulse CPI method with density gradients.

The remainder of this paper is organized as follows. The general concept of using density down-ramps is discussed in Sec. II. The analytical expressions for the wakefield driven on a density ramp are derived in Sec. III. Section IV presents the numerical results, in which the motion of test particles are tracked in 3D in the analytically specified fields of the laser pulses and wakes. A discussion of the results is given in Sec. V. Also included is an appendix that discusses beam loading.

II. DENSITY DOWN-RAMPS

A density down-ramp can enhance the number of trapped and focused electrons by two effects: (1) a decrease in density shifts the position of an electron forward in phase with respect to the wakefield and (2) a decrease in density decreases the phase velocity of the wake, thus providing a lower threshold for injection. Consider a change in density from n_i to n_f ($n_i > n_f$) over a length L_t , and assume that the trapped electron and laser are all moving in the forward direction (z) with velocity near c . The phases of the electron before and after the transition are given by $\psi_i = k_{pi}\zeta$ and $\psi_f = k_{pf}\zeta$, respectively, assuming that the slippage between the electron and drive laser pulse is small over L_t (ζ is approximately constant), where $\zeta = z - ct$ is the position of the electron behind the drive pulse ($\zeta < 0$ behind the drive pulse) and $k_{pi} = \omega_{pi}/c$ and $k_{pf} = \omega_{pf}/c$ are the plasma wave numbers evaluated at n_i and n_f , respectively. The change in phase of the electron after the density transition is $\Delta\psi = \psi_i - \psi_f$ —i.e.,

$$\Delta\psi = \psi_i [1 - (n_f/n_i)^{1/2}] \approx \psi_i (\Delta n/2n_i), \quad (1)$$

assuming $\Delta n = n_i - n_f \ll n_i$. Hence, the change in density required to shift an electron forward in phase by a small

amount (e.g., $\Delta\psi \sim \pi/4$) is $\Delta n/n_i = 2(\Delta\psi/\psi_i) = 2(\Delta\psi/k_{pi}\zeta)$. Note that rephasing becomes easier (a smaller $\Delta n/n_i$ is required) with increasing distance behind the driver (larger $|\zeta|$). Hence, rephasing is more efficient for the three-pulse CPI configuration than for two-pulse CPI, assuming the injection point for three-pulse CPI is behind the first wake period.

If the injection (pulse collision) point was to occur on the down-ramp (as opposed to prior to it), then trapping could be further enhanced due to the decrease in phase velocity of the wake on the down-ramp. The wake phase velocity v_p can be calculated from the wake phase $\psi = k_p(z)(z - ct)$ via $v_p/c = -(\partial\psi/\partial ct)/(\partial\psi/\partial z)$. This gives

$$v_p/c = 1/(1 + k_p^{-1}\zeta dk_p/dz), \quad (2)$$

where $dk_p/dz = (k_p/2n)dn/dz$. Since $\zeta < 0$ behind the drive pulse, the phase velocity decreases on a density down-ramp ($dn/dz < 0$). Note that this effect becomes more pronounced the larger the distance behind the driver. Thus, the reduction in phase velocity due to the down-ramp is potentially more effective for three-pulse CPI than for two-pulse CPI. Eventually, even in the absence of an injection pulse, the down-ramp leads to wave breaking and injection for a sufficiently large distance behind the pump pulse [7], assuming that the wake amplitude does not damp.

III. PLASMA RESPONSE

The cold fluid equations, describing the evolution of the plasma density n , the normalized electron fluid momentum $\mathbf{u} = \mathbf{p}/mc$, the normalized electrostatic potential $\phi = e\Phi/mc^2$, and the normalized vector potential $\mathbf{a} = e\mathbf{A}/mc^2$, are given by

$$\partial n/\partial ct + \nabla \cdot (n\mathbf{u}/\gamma) = 0, \quad (3)$$

$$\partial(\mathbf{u} - \mathbf{a})/\partial ct = \nabla(\phi - \gamma), \quad (4)$$

$$\nabla^2 \phi = k_{p0}^2 [n/n_{00} - n_0(z)], \quad (5)$$

$$(\nabla^2 - \partial^2/\partial ct^2)\mathbf{a} = k_{p0}^2 (n/n_{00})\mathbf{u}/\gamma + \nabla\partial\phi/\partial ct, \quad (6)$$

where $\gamma = (1 + u^2)^{1/2}$, $n_0(z)$ is the initial density profile, $k_{p0} = (4\pi n_{00}e^2/mc^2)^{1/2}$ is the plasma wave number evaluated at constant density $n_{00} = n_0(0)$, and $\nabla \times (\mathbf{u} - \mathbf{a}) = \mathbf{0}$ has been assumed along with the gauge condition $\nabla \cdot \mathbf{a} = 0$.

These equations will be solved order by order with respect to the small parameter $|a_L| \ll 1$, which is the normalized amplitude of the laser field. To first order, all quantities are small except for $\mathbf{u}_1 \approx \mathbf{a}_L$. The first-order quantities are given by

$$\partial n_1/\partial ct + \nabla \cdot (n_0\mathbf{u}_1) = 0, \quad (7)$$

$$\partial(\mathbf{u}_1 - \mathbf{a}_L)/\partial ct = \nabla\phi_1, \quad (8)$$

$$\nabla^2 \phi_1 = k_{p0}^2 n_1/n_{00}, \quad (9)$$

which can be combined to yield

$$\nabla^2 \partial^2 \phi_1/\partial ct^2 + \nabla \cdot [k_{p0}^2 (\nabla\phi_1 + \partial\mathbf{a}_L/\partial ct)] = 0, \quad (10)$$

where $k_p^2 = k_{p0}^2 n_0(z)/n_{00}$. Since the primary contributions to the first-order quantities are on the fast time scale—i.e., $\phi_1 \sim \exp[ik(z-ct)]$, where k is the laser wave number—the first-order quantities scale as $\phi_1 \sim k_p^2 a_L / (k^4 r_0 L_t)$, $n_1/n_{00} \sim a_L / (k^2 r_0 L_t)$, $(u_1 - a_L)_z \sim k_p^2 a_L / (k^4 r_0 L_t)$, and $(u_1 - a_L)_\perp \sim k_p^2 a_L / (k^5 r_0^2 L_t)$, where L_t is the scale length of the axial density transition, $\partial k_p^2 / \partial z \sim k_p^2 / L_r$, and r_0 is the scale length of the transverse gradient. Since $k/k_p \gg 1$, $kL_t \gg 1$, and $kr_0 \gg 1$, all first-order quantities will be neglected except for $\mathbf{u}_1 \approx \mathbf{a}_L$.

To second order,

$$\partial n_2 / \partial ct + \nabla \cdot (n_0 \mathbf{u}_2) = 0, \quad (11)$$

$$\partial (\mathbf{u}_2 - \mathbf{a}_2) / \partial ct = \nabla (\phi_2 - a_L^2 / 2), \quad (12)$$

$$\nabla^2 \phi_2 = k_{p0}^2 n_2 / n_{00}, \quad (13)$$

$$(\nabla^2 - \partial^2 / \partial ct^2) \mathbf{a}_2 = k_p^2(z) \mathbf{u}_2 + \nabla \partial \phi_2 / \partial ct, \quad (14)$$

along with $\nabla \cdot \mathbf{a}_2 = 0$. These equations can be combined to yield

$$(\partial^2 / \partial ct^2 + k_p^2) \nabla \phi_2 - k_p^2 \nabla a_L^2 / 2 = (\nabla^2 - \partial^2 / \partial ct^2 - k_p^2) \partial \mathbf{a}_2 / \partial ct. \quad (15)$$

In both the uniform plasma limit ($k_p^2 = k_{p0}^2$) and the 1D limit ($\nabla_\perp = 0$), $\mathbf{a}_2 = 0$.

The above equation can be solved in the limits $k_p L_t \gg 1$ and $k_p r_0 \gg 1$ by assuming an ordering $|\phi_2| \gg |a_{\perp 2}| \gg |a_{z2}|$. As is shown below, these terms scale as $a_{\perp 2} \sim \phi_2 / (k_p^2 r_0 L_t)$ and $a_{z2} \sim \phi_2 / (k_p^3 r_0^2 L_t)$. This last scaling follows from $\nabla \cdot \mathbf{a}_2 = 0$ —i.e., $a_{z2} \sim a_{\perp 2} / (k_p r_0)$. In the following, an averaging over the fast laser frequency is assumed such that the time and axial derivatives scale as $\partial / \partial ct \sim \partial / \partial z \sim k_p$. Taking the axial component of the above equation yields, to leading order,

$$\left(\frac{\partial^2}{\partial ct^2} + k_p^2 \right) \frac{\partial \phi_2}{\partial z} \approx k_p^2(z) \frac{\partial}{\partial z} \left(\frac{a_L^2}{2} \right), \quad (16)$$

where a term of order $k_p^3 a_{z2} \sim \phi_2 / (r_0^2 L_t)$ has been neglected. This determines the axial wakefield $E_z \sim \partial \phi_2 / \partial z$, neglecting terms of order $1 / (k_p^2 r_0 L_t)$ or higher. To determine the electromagnetic contribution to the wake ($a_{\perp 2}$), the transverse component of Eq. (15) is operated on by $\partial / \partial z$, which yields

$$\frac{\partial}{\partial z} \left[\left(\nabla^2 - \frac{\partial^2}{\partial ct^2} - k_p^2 \right) \frac{\partial a_{x2}}{\partial ct} \right] = \left(\frac{\partial k_p^2}{\partial z} \right) \frac{\partial}{\partial x} \left(\phi_2 - \frac{a_L^2}{2} \right). \quad (17)$$

Scaling the operators in the above equation implies $a_{x2} \sim \phi_2 / (k_p^2 r_0 L_t)$. Hence, the transverse electric field of the wake is given to leading order by $E_x \sim \partial \phi_2 / \partial x$, where terms of order $1 / (k_p L_t)$ or higher are neglected.

Consider the wakefields being driven by a forward-going pump laser pulse ($i=0$) and a backward-going injection laser

pulse ($i=1$), the fields of which are described by the normalized vector potentials $\mathbf{a}_i = e \mathbf{A}_i / m_e c^2$. The wake driven by the beating of the pump and injection pulse will be neglected, as discussed in Refs. [16,17]. The transverse laser field (linearly polarized in the x direction and propagating along the z axis) is given by [20]

$$a_{xi}(r, \zeta_i) = \hat{a}_i(r, \zeta_i) \cos \psi_i, \quad (18)$$

with

$$\hat{a}_i(r, \zeta_i) = a_i(r/r_{si}) \exp(-r^2/r_{si}^2) \sin(\pi \zeta_i / L_i), \quad (19)$$

for $-L_i < \zeta_i < 0$ and zero otherwise, where $\zeta_0 = z - \beta_{g0} ct$ (forward-comoving coordinate), $\zeta_1 = -z - \beta_{g1} ct$ (backward-comoving coordinate), $\beta_{gi} = \eta_i$ is the linear group velocity, $\beta_{\phi i} = \eta_i^{-1}$ is the linear phase velocity, $\eta_i = (1 - \omega_p^2 / \omega_i^2 - 4 / k_i^2 r_i^2)^{1/2}$ is the plasma index of refraction, $\psi_i = k_i(z - \beta_{\phi i} ct) + \alpha_i r^2 / r_{si}^2 + \alpha_i - \tan^{-1} \alpha_i$ is the phase, $k_i = \omega_i / (\beta_{\phi i} c)$ is the wave number, ω_i is the frequency in vacuum, $r_{si}(z) = r_i [1 + \alpha_i(z)]^{1/2}$ is the spot size, r_i is the spot size at waist (here chosen to be $z = Z_{fi}$), $\alpha_i(z) = (z - Z_{fi})^2 / Z_{Ri}^2$, $Z_{Ri} = k_i \eta_i r_i^2 / 2$ is the Rayleigh length, L_i is the pulse length, and a constant has been omitted in the definition of ψ_i that represents the initial position and phase of the laser pulse. The axial component of the laser field is specified via $\nabla \cdot \mathbf{a}_i = 0$. Keeping only the leading-order contributions gives

$$a_{zi}(r, \zeta_i) \approx 2x [\hat{a}_i(r, \zeta_i) / (k_i r_{si}^2)] (\sin \psi_i - \alpha_i \cos \psi_i). \quad (20)$$

Included in the simulations presented below are the wakefields generated by both the pump and injection laser pulses. For linear polarization and assuming $k_p r_0 \gg 1$ and $k_p L_t \gg 1$ —i.e., a large laser spot and a slowly varying density transition—the normalized electric field of the wakefield $k_{p0} \mathbf{E}_i / E_0 = -\nabla \phi_{2i}$ is given by

$$[\partial^2 / \partial \zeta_i^2 + k_p^2(z)] k_{p0} \mathbf{E}_i / E_0 \approx k_p^2(z) \nabla \hat{a}_i^2 / 4, \quad (21)$$

where $E_0 = mc^2 k_{p0} / e$ is the cold nonrelativistic wave-breaking field evaluated at fixed density n_{00} and independent variables ζ_i and z have been used. Note that a time averaging has been performed over the fast laser oscillation (laser frequency)—i.e., $\langle \hat{a}_i^2 \cos^2 \psi_i \rangle = \hat{a}_i^2 / 2$. The axial component of Eq. (21) follows directly from Eq. (16), whereas the transverse component represents the leading-order contribution to E_\perp , neglecting corrections of order $1 / (k_p L_t)$ or higher. Assuming that \hat{a}_i^2 is a slowly varying function of z —i.e., $|\partial \hat{a}_i^2 / \partial \zeta_i| \gg |\partial \hat{a}_i^2 / \partial z|$ —the solution to Eq. (21) is

$$\begin{aligned} \mathbf{E}_i(r, \zeta_i) / E_0 = & - [k_p(z) / 4 k_{p0}] \int_0^{\zeta_i} d\zeta'_i \sin[k_p(z)(\zeta_i - \zeta'_i)] \\ & \times (\partial / \partial \zeta'_i + \nabla_\perp) \hat{a}_i^2(r, \zeta'_i), \end{aligned} \quad (22)$$

where a term proportional to $\partial \hat{a}_i^2 / \partial z$ has been neglected inside the integrand, which neglects additional terms of order $L_i / Z_{Ri} \sim 1 / (k k_p r_0^2) \ll 1$. Specifically, Eq. (21) yields the electric field generated inside the pulse ($-L_i < \zeta_i < 0$),

$$\frac{\mathbf{E}_{ri}}{E_0} = \frac{a_i^2}{2} \frac{r_i^2 r}{k_{p0} r_{si}^4} e^{-2r^2/r_{si}^2} \times \left[1 + \frac{(4\pi^2/k_p^2 L_i^2) \cos(k_p \xi_i) - \cos(2\pi \xi_i/L_i)}{(1 - 4\pi^2/k_p^2 L_i^2)} \right], \quad (23)$$

$$\frac{\mathbf{E}_{zi}}{E_0} = \frac{k_p}{k_{p0}} \frac{a_i^2}{8} \frac{r_i^2}{r_{si}^2} e^{-2r^2/r_{si}^2} \left[\frac{(4\pi^2/k_p^2 L_i^2) \sin(k_p \xi_i) - \sin(2\pi \xi_i/L_i)}{(1 - 4\pi^2/k_p^2 L_i^2)} \right], \quad (24)$$

and behind the pulse ($\xi_i < -L_i$),

$$\frac{\mathbf{E}_{ri}}{E_0} = a_i^2 \frac{r_i^2 r}{k_{p0} r_{si}^4} e^{-2r^2/r_{si}^2} \left(\frac{4\pi^2}{k_p^2 L_i^2} \right) \frac{\sin[k_p(\xi_i + L_i/2)] \sin(k_p L_i/2)}{(1 - 4\pi^2/k_p^2 L_i^2)}, \quad (25)$$

$$\frac{\mathbf{E}_{zi}}{E_0} = -\frac{k_p}{k_{p0}} \frac{a_i^2}{4} \frac{r_i^2}{r_{si}^2} e^{-2r^2/r_{si}^2} \left(\frac{4\pi^2}{k_p^2 L_i^2} \right) \frac{\cos[k_p(\xi_i + L_i/2)] \sin(k_p L_i/2)}{(1 - 4\pi^2/k_p^2 L_i^2)}. \quad (26)$$

For the resonant case $L_i = \lambda_p$, which corresponds to a condition close to maximum wakefield generation, inside the pulse,

$$\frac{\mathbf{E}_{ri}}{E_0} = \frac{a_i^2}{2} \frac{r_i^2 r}{k_{p0} r_{si}^4} e^{-2r^2/r_{si}^2} [1 - \cos(k_p \xi_i) - (k_p \xi_i/2) \sin(k_p \xi_i)], \quad (27)$$

$$\frac{\mathbf{E}_{zi}}{E_0} = -\frac{k_p}{k_{p0}} \frac{a_i^2}{8} \frac{r_i^2}{r_{si}^2} e^{-2r^2/r_{si}^2} [\sin(k_p \xi_i)/2 - (k_p \xi_i/2) \cos(k_p \xi_i)], \quad (28)$$

and behind the pulse,

$$\frac{\mathbf{E}_{ri}}{E_0} = \frac{\pi a_i^2}{2} \frac{r_i^2 r}{k_{p0} r_{si}^4} e^{-2r^2/r_{si}^2} \sin(k_p \xi_i), \quad (29)$$

$$\frac{\mathbf{E}_{zi}}{E_0} = -\frac{k_p}{k_{p0}} \frac{\pi a_i^2}{8} \frac{r_i^2}{r_{si}^2} e^{-2r^2/r_{si}^2} \cos(k_p \xi_i). \quad (30)$$

Note that for high laser intensities ($|a_i| > 1$), this model becomes inaccurate. To describe the nonlinear regime in 3D, as well as other nonlinear effects such as beam loading, requires self-consistent simulations (e.g., particle-in-cell codes), which is beyond the scope of this paper.

IV. SIMULATION RESULTS

The effect of density down-ramps on the bunch quality in the colliding pulse injector was studied using a 3D particle tracking code, which evolves the motion of a group of test particles in analytically specified fields. Included in the simulations are the electromagnetic fields of the laser pulses, as determined from the vector potentials given by Eqs. (18)–(20). The wakefields from the pump and injection laser pulses are given by Eqs. (23)–(26). The ion density profile is assumed to be of the form

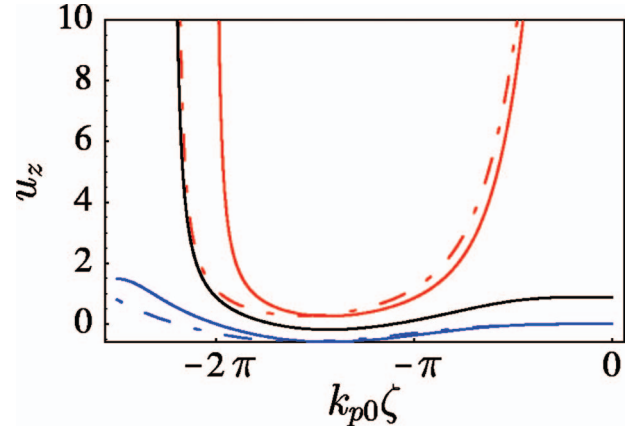


FIG. 1. (Color) Phase-space plot showing cold-fluid orbit for $n_0/n_{00}=1$ (blue solid line), $n_0/n_{00}=0.7$ (blue dot-dashed line), trapped and focused orbit for $n_0/n_{00}=1$ (red solid line), $n_0/n_{00}=0.7$ (red dot-dashed line), and orbit of an electron in a trapped but defocusing region of the wakefield for $n_0/n_{00}=1$ (black solid line), with laser parameters $L_0 = \lambda_{p0}$ and $a_0 = 1$.

$$\frac{n_0(z)}{n_{00}} = 1 - \frac{\tau_t}{2} \left[1 + \tanh\left(\frac{z - z_t}{L_t}\right) \right], \quad (31)$$

where n_{00} is the ion density before the density drop-off ($z < z_t$), z_t is the location of the transition, and $\tau_t = \Delta n_0/n_{00}$ is the relative change of density.

In the following simulations, the plasma was modeled by a group of test electrons initially at rest and loaded randomly in a three-dimensional spatial region of length λ_p and transverse radius $\lambda_p/2$, uniformly about the z axis, corresponding to a volume $V_0 = \pi \lambda_p^3/4$. This spatial region was chosen to be ahead of the pump laser pulse and timed with respect to the initial position of the injection pulse such that, when the two pulses collide, the test electrons fill the entire region in which trapping may occur. After the collision, various properties of the trapped electron bunch were monitored as a function of propagation time, such as the mean energy, the energy spread, the root-mean-square (rms) bunch length, rms bunch radius, and the trapping fraction. Here, the trapping fraction is defined as N_b/N_s , where N_b is the number of test electrons in the bunch and N_s the total number of test electrons in the simulation. A quasi-1D configuration with $r_i \approx \lambda_p$ was chosen, such that most of the injected electrons, although in a defocusing region of the accelerating wave, will only slowly depart transversely from their initial on-axis location. A density down-ramp will then rephase those electrons onto a trapped and focused orbit. This is shown in Fig. 1, where the cold fluid orbit and trapped and focused orbit are both shown for an initial density n_{00} and another density 30% smaller. Note that the focusing region has been extended farther behind the pump pulse. The simulations were carried out for normalized laser-plasma parameters $a_0 = 1$, $\omega_0/\omega_{p0} = 50$, and $L_0 = \lambda_{p0}$ or $9\lambda_{p0}/8$, $\omega_1/\omega_{p0} = 50$, and $L_1 = \lambda_{p0}/2$. Parameter scans were performed for the injection pulse normalized vector potential a_1 and for the parameters corresponding to the density ramp such as the length L_t , the center of the transition z_t , and the relative change of density τ_t .

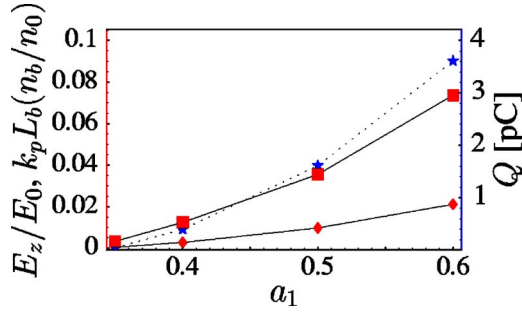


FIG. 2. (Color online) Bunch charge Q in pC (right vertical axis, stars), $k_p L_b (n_b/n_0)$ (left vertical axis, squares), and normalized axial electric field E_z/E_0 (left vertical axis, points) generated by the electron bunch alone (here the laser contribution is not included) versus a_1 with $\lambda_0=0.8 \mu\text{m}$, $L_0=9\lambda_{p0}/4$, $r_0=\lambda_{p0}=40 \mu\text{m}$, $a_0=1$, homogeneous plasma—e.g., no density ramp and $ct=47k_{p0}^{-1}\approx 300 \mu\text{m}$ after injection.

Figure 2 shows the resulting electron beam characteristics produced in a uniform plasma without the use of a plasma density gradient [16,17]. The total charge in the bunch Q was estimated from the trapping fraction f_{tr} (the fraction of the initial electrons that remain on trapped and focused orbits) by $Q=en_0 f_{\text{tr}} V_0$. The bunch density was calculated assuming a square beam profile using the relationships between the length, radius, and corresponding rms quantities; e.g., $L_b=2\sqrt{3}\sigma_z$ is the full beam length, σ_z the rms beam length, $r_b=2\sigma_r$ the beam radius, and σ_r the beam rms radius. As shown in Fig. 2, the typical value of the charge injected is on the order ~ 4 pC. Note also that for high bunch charge, beam loading may become important (see the Appendix for further details). For a uniform beam profile $n_b(r, \zeta)=n_b\Theta(r_b-r)\Theta(-\zeta)\Theta(\zeta+L_b)$ of radius r_b and length L_b , where Θ is a step function, the amplitude of the perturbed density and the axial electric field of the bunch-induced wake is found to be at the back of the bunch [16,17,21,22],

$$\delta n/n_0 \approx -(k_p L_b)^2 (n_b/n_0)/2, \quad (32)$$

$$E_z/E_0 \approx k_p L_b (n_b/n_0) F_R(r), \quad (33)$$

assuming $k_p L_b \ll 1$, $\delta n/n_0 \ll 1$, and $E_z/E_0 \ll 1$, where the radial profile function is $F_R(r)=1-k_p r_b K_1(k_p r_b) I_0(k_p r)$ for $r < r_b$. Here I_0 and K_1 are modified Bessel functions. For a narrow beam $k_p^2 r_b^2 \ll 1$, and along the axis, $F_R(r=0) \approx [0.308 - 0.5 \ln(k_p r_b)] k_p^2 r_b^2$. For $k_p L_b (n_b/n_0) \approx 1$ the linear wake approximation becomes inaccurate and nonlinear methods must be used. Another parameter of interest is a comparison of the wakefield intensity produced by the laser pulse with respect to the wake induced by the beam itself. The latter is required to be much smaller. Using Eq. (30) together with Eq. (33) yields an approximated ratio

$$\alpha_1 \approx \frac{8 k_p L_b n_b}{\pi a_0^2 n_0} F_R(0) \ll 1, \quad (34)$$

which is valid for a laser beam close to the resonant condition $L \approx \lambda_p$. For the case of Fig. 2 beam loading is a negligible effect.

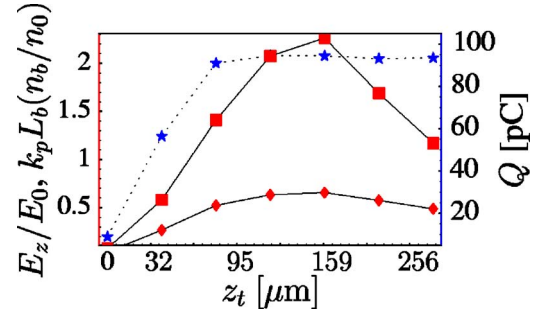


FIG. 3. (Color online) Bunch charge Q in pC (right vertical axis, stars), $k_p L_b (n_b/n_0)$ (left vertical axis, squares), and normalized axial electric field E_z/E_0 (left vertical axis, points) generated by the electron bunch alone versus z_t with $\lambda_0=0.8 \mu\text{m}$, $L_0=9\lambda_{p0}/4$, $r_0=\lambda_{p0}=40 \mu\text{m}$, $a_0=1$, $a_1=0.5$, $L_t=\lambda_{p0}$, $\tau_t=30\%$, and $ct=147k_{p0}^{-1}\approx 935 \mu\text{m}$ after injection.

Figure 3 shows the amount of charge in the trapped and focused region of the plasma wave as a function of the density down-ramp center z_t for the laser-plasma parameters: $a_0=1$, $\omega_0/\omega_{p0}=50$, $L_0=9\lambda_{p0}/8$, $a_1=0.5$, $\omega_1/\omega_{p0}=50$, $L_1=\lambda_{p0}/2$, $L_t=\lambda_{p0}$, $\tau_t=30\%$, and $\omega_{p0}t=147$ after injection. Here λ_{p0} corresponds to the plasma wavelength prior to the density transition. The total charge is increasing temporarily up to a plateau region reached at about $k_{p0}z_t=4\pi$. As mentioned above, Fig. 1 shows the phase shift of the trapped and focused region after passing through the density transition [according to Eq. (1)] as well as a typical orbit of an electron lying in the defocusing region. The latter electrons will circulate along this path towards the high-energy region and will cross the extended focusing region of the plasma wave at some later time after injection. Delaying the density transition until those electrons reach the phase $\psi_f \approx 2\pi$ will allow for rephasing of maximum amount of charge. In Fig. 3, a charge per bunch enhancement by a factor of ~ 50 is shown. In this case beam loading may become important; e.g., the bunch-induced wakefield E_z/E_0 becomes comparable to the wake generated by the drive laser pulse alone. Nonlinear beam loading will most likely reduce the bunch quality (fraction trapped, average energy, etc.). Note that the oscillation shown in Fig. 3 for the electric field E_z/E_0 as well as for the beam density $k_p L_b (n_b/n_0)$ may be attributed to the extra focusing provided to the rephased electrons by the plasma wave.

Figure 4 plots the parameter $k_p L_b (n_b/n_0)$ (which is used as an indicator for the estimation of the validity of the linear regime in the calculation of beam loading), the electric field E_z/E_0 induced by the electron beam alone, and the charge trapped as a function of the injection laser strength a_1 for the same laser-plasma parameters as of Fig. 3 except for $k_{p0}z_t=12\pi$. The latter correspond to the region of Fig. 3 where maximum trapping is achieved. Comparing Fig. 2 with Fig. 4 shows a lower trapping threshold as expected ($a_{1 \text{ min}} \approx 0.35$ versus 0.15). The electron beam remains compact as shown in Fig. 5. The rms bunch radius σ_r , and rms bunch duration σ_z are on the order of a few percent of the plasma wavelength λ_{p0} . For a plasma wavelength on the order of $10 \mu\text{m}$, this implies that <1 fs (i.e., attosecond scale) bunches can be produced. The bunch normalized emittance is approximated

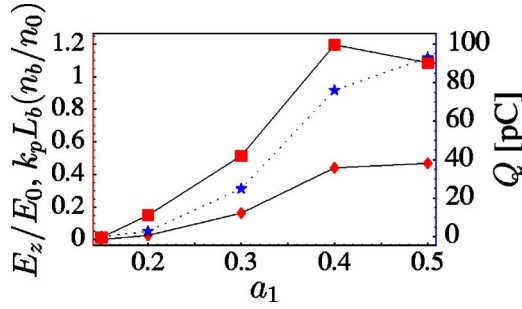


FIG. 4. (Color online) Bunch charge Q in pC (right vertical axis, stars), $k_p L_b(n_b/n_0)$ (left vertical axis, squares) and normalized axial electric field E_z/E_0 (left vertical axis, points) generated by the electron bunch alone versus a_1 with $\lambda_0=0.8 \mu\text{m}$, $L_0=9\lambda_{p0}/4$, $r_0=\lambda_{p0}=40 \mu\text{m}$, $a_0=1$, $z_t=240 \mu\text{m}$, $L_t=\lambda_{p0}$, $\tau_t=30\%$, and $ct=147k_{p0}^{-1}=935 \mu\text{m}$ after injection.

as $\epsilon_{\perp}=\gamma_0\beta_0\sqrt{\langle x^2\rangle\langle x'^2\rangle}\approx\sqrt{\langle x^2\rangle\langle u_x^2\rangle}$, where $u_0=\gamma_0\beta_0\approx\gamma_0$ is the axial momentum of the electron bunch. For the case of Fig. 5, the emittance is typically small—e.g., $\lambda_{p0}=40 \mu\text{m}$ ($n_{00}=6.9\times 10^{17} \text{cm}^{-3}$)—and implies $\epsilon_{\perp}<0.8 \text{mm mrad}$ for an average kinetic energy of $\approx 23 \text{MeV}$. The energy spread $\Delta\gamma/\gamma$ is on the order of a few percent.

A 1D analysis of the dephasing length [1] (which is the typical length required for a trapped electron to outrun the plasma wave, resulting in maximum energy gain) gives $L_d\approx\gamma_p^2\lambda_p$, where $\gamma_p=(1-\beta_p^2)^{1/2}$ is the plasma wave relativistic factor and $\beta_p\approx\beta_{g0}$ is the plasma wave normalized phase

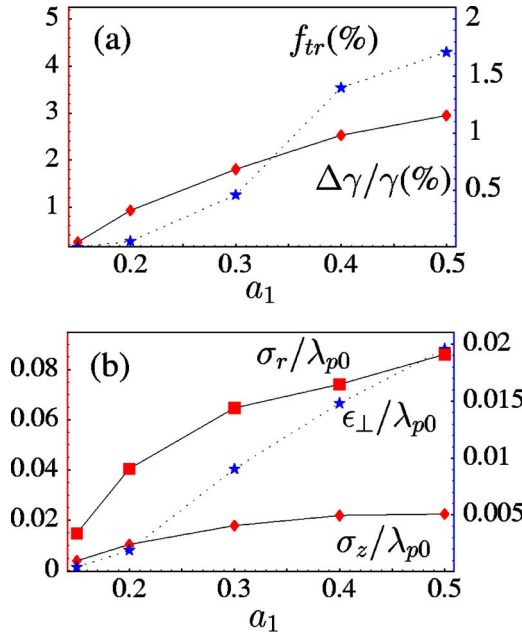


FIG. 5. (Color online) Trapped bunch parameters versus a_1 (for two collinear, counterpropagating laser pulses with equal polarization, $a_0=1$, $\omega_0/\omega_{p0}=50$, $L_0=9\lambda_{p0}/8$, $\omega_1/\omega_{p0}=50$, $L_1=\lambda_{p0}/2$, $k_{p0}z_t=12\pi$, $k_{p0}L_t=2\pi$, $\tau_t=30\%$, and $ct=147k_{p0}^{-1}$). (a) Trapping fraction f_{tr} (right vertical axis) and relative energy spread $\Delta\gamma/\gamma$ (left vertical axis). (b) Bunch length σ_z/λ_{p0} (left vertical axis), rms radius σ_r/λ_{p0} (left vertical axis), and normalized transverse rms emittance $\epsilon_{\perp}/\lambda_{p0}$ (right vertical axis).

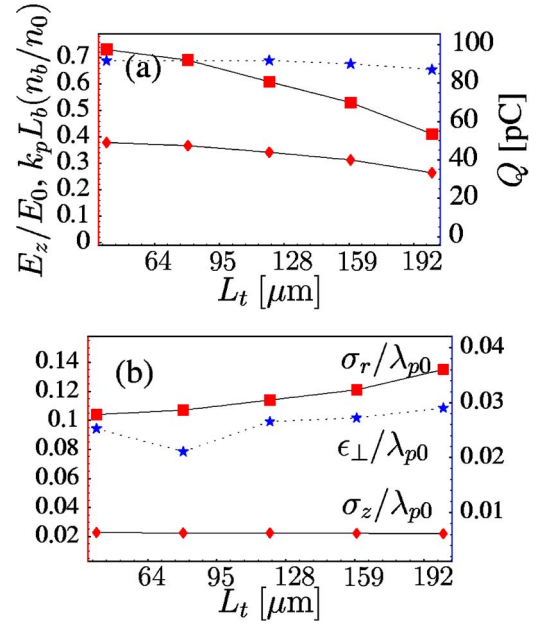


FIG. 6. (Color online) (a) Bunch charge Q in pC (right vertical axis, stars), $k_p L_b(n_b/n_0)$ (left vertical axis, squares), and normalized axial electric field E_z/E_0 (left vertical axis, points) generated by the electron bunch alone. (b) Bunch length σ_z/λ_{p0} (left vertical axis), rms radius σ_r/λ_{p0} (left vertical axis), and normalized transverse rms emittance $\epsilon_{\perp}/\lambda_{p0}$ (right vertical axis) versus L_t for the laser-plasma parameters: $\lambda_0=0.8 \mu\text{m}$, $L_0=9\lambda_{p0}/4$, $r_0=\lambda_{p0}=40 \mu\text{m}$, $a_0=1$, $a_1=0.5$, $z_t=280 \mu\text{m}$, $\tau_t=30\%$, and $ct=147k_{p0}^{-1}=935 \mu\text{m}$ after injection.

velocity, which is approximately equal to the laser group velocity in the linear regime. For an underdense plasma $\omega_p/\omega_0\ll 1$, $\gamma_p\approx\omega_0/\omega_p$ which corresponds to $L_d\sim 10 \text{cm}$ for $n_0\sim 7\times 10^{17} \text{cm}^{-3}$. Furthermore, in 3D, the Rayleigh length $Z_R\approx k_0r_0^2/2$ (which is the characteristic distance for laser diffraction) must be compared to the dephasing length and is found to be on the order 4 cm. The beam parameters shown in Fig. 5 are evaluated only after a propagation distance on the order 1 mm. Therefore, the beam quality is expected to improve over longer acceleration distances (increase of kinetic energy, lower energy spread, etc.), up to the limits imposed by dephasing and/or diffraction.

Figure 6(a) plots the parameter $k_p L_b(n_b/n_0)$, bunch charge Q , and bunch-induced axial electric field E_z/E_0 as a function of the density transition length L_t . Figure 6(a) shows a small effect on the beam quality; e.g., the trapping fraction remains mainly unchanged. The small increase in bunch radius together with the emittance [Fig. 6(a)] can be explained by the fact that a long density transition implies that the electron beam remains for a longer period of time in a defocusing phase. The requirement on the transition length L_t is to be smaller than the typical distance it takes an electron to outrun the plasma wave. For the laser-plasma parameters used in this paper, $Z_R<L_d$ and $k_p^{-1}\ll L_t\ll Z_R$. This demonstrates the feasibility of using negative plasma density gradients in laboratory experiments as a means for rephasing trapped but unfocused electrons.

Figure 7 shows the trapped bunch charge and corresponding beam loading parameters as a function of the relative

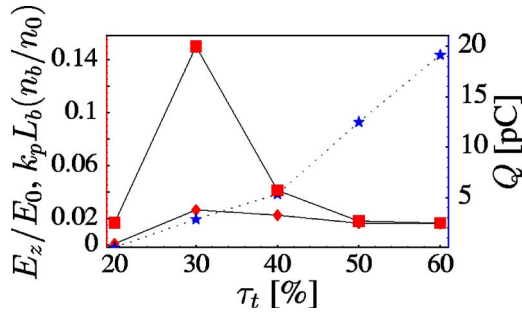


FIG. 7. (Color online) Bunch charge Q in pC (right vertical axis, stars), $k_p L_b(n_b/n_0)$ (left vertical axis, squares) and normalized axial electric field E_z/E_0 (left vertical axis, points) generated by the electron bunch alone versus τ_t with $\lambda_0=0.8 \mu\text{m}$, $L_0=r_0=\lambda_{p0}=40 \mu\text{m}$, $a_0=1$, $a_1=0.2$, $z_i=240 \mu\text{m}$, $L_i=40 \mu\text{m}$, and $ct=147k_{p0}^{-1}\approx 935 \mu\text{m}$ after injection.

change of density τ_t for the laser-plasma parameters $\lambda_0=0.8 \mu\text{m}$, $L_0=r_0=\lambda_{p0}=40 \mu\text{m}$, $a_0=1$, $a_1=0.2$, $z_i=240 \mu\text{m}$, $L_i=40 \mu\text{m}$, and $ct=147k_{p0}^{-1}\approx 935 \mu\text{m}$ after injection. Note that $a_1=0.2$ is found to be close to the trapping threshold for $\tau_t\approx 25\%$, and by increasing τ_t , the trapped charge in the bunch became as high as $Q=20$ pC for $\tau_t=60\%$. Consequently, for such values of τ_t , the trapping threshold is lower than $a_1=0.2$, which is an order of magnitude smaller than the laser strength required in ponderomotive injection schemes [11]. Another possible interesting regime would be to lower the drive pulse strength instead of the injection pulse. Using $k_p L_0=k_p r_0=k_p r_1=2\pi$ along with $a_1=0.5$ and $k_p L_1=4\pi$ (a length far from the resonant condition in order to minimize the injection wake which could interfere with the wake generated by the drive pulse itself for the case of a modest value of a_0), combined with a long taper length $k_p z_i > 5\pi$ (to allow maximum injection; e.g., see Fig. 3) and $\tau_t=30\%$, may provide a threshold as low as $a_0=0.8$.

V. CONCLUSION

Plasma density down-ramps have been proposed as a method for improving electron bunch quality in laser injection schemes. A decrease in density implies an increase in plasma wavelength, which can shift a relativistic electron from the defocusing to the focusing region of the accelerating wakefield. Also, a decrease in density leads to a decrease in wake phase velocity, which can lower the trapping threshold. The specific method of two-pulse CPI was examined using a 3D test particle tracking code. Various properties of the trapped and focused bunch were studied as a function of the ramp and laser parameters. For example, it was found that a density down-ramp of 30% change in density with $L_i=\lambda_p$ increased the trapped and focused charge from 0 pC (no ramp) to 25 pC (with ramp) for an injection pulse intensity of $a_1=0.3$ and from <2 pC to 100 pC (which is near the beam loading limit) for $a_1=0.5$. Furthermore, no degradation of overall bunch parameters was observed compared to the uniform plasma case. The bunch duration was found to be typically on the order of a few percent of the plasma wavelength, which implies formation of attosecond electron

bunches for short plasma wavelengths. The trapped bunch quality was found to depend only weakly on the length of the ramp, indicating that the use of experimentally feasible ramps with $L_i \gg \lambda_p$ can be effective in enhancing the trapped bunch. Since the use of down-ramps increases the number of trapped and focused electrons, the overall trapping threshold for electron injection into the plasma wave is lowered, which allows the production of trapped bunches with lower-intensity laser pulses.

One limitation of the approach used in this research is that it relies on test particle simulations in which the fields (lasers and wakes) were specified analytically. Specifically, analytical expressions were used for the wakefield valid to second order in the normalized laser field a_i^2 . This model becomes inaccurate as a_i^2 approaches and exceeds unity, and self-consistent simulations, such as using particle-in-cell or fluids codes, are required in this nonlinear regime. A second approximation used in the test particle simulations is the neglect of the wake generated by the trapped bunch—i.e., neglect of beam loading. These test particle simulations indicate that the colliding pulse trapping mechanism is rather robust; i.e., it is easy to trap electrons up to beam loading limit. Again, to fully assess the utility of the colliding pulse injection in the high-charge limit, self-consistent simulations are required.

It should be noted that although this study was restricted to the two-pulse colliding-pulse configuration, rephasing and enhancement of the trapped bunch quality by using density transitions is a general method that can be applied to a wide variety of plasma-based accelerators. In general, the relative phase of the bunch in the wake can be repositioned by adjusting the plasma density. As discussed above, the change in density required to shift an electron forward in phase by a small amount is $\Delta n/n_i=2(\Delta\psi/k_{pi}\zeta)$. Note that rephasing becomes easier (a smaller $\Delta n/n_i$ is required) with increasing distance behind the driver (larger $|\zeta|$). Hence, rephasing is more efficient for the bunches trapped in buckets further behind the driver. Typically, only a small change of density is required to shift the phase a significant fraction of a plasma period. Since the wake amplitude is a relatively weak function of density, rephasing can be accomplished by small changes in the density without significantly degrading the accelerating field of the wake. Furthermore, provided that the plasma density transition occurs over a length (or time) that is short compared to the dephasing length of the electron in the wake (or the synchrotron period for a trapped electron in the wake), the rephasing (shifting of the wake relative to the electron) occurs virtually instantaneously with respect to the electron dynamics. Since the dephasing length of a relativistic electron in a plasma wake is relatively long, $L_d\approx\lambda_p^3/\lambda^2$, experimentally producing a density transition with $L_i\ll L_d$ is readily achievable, which in turn leads to a near-instantaneous rephasing of the electrons in the wake.

ACKNOWLEDGMENTS

This work was performed under the auspices the U.S. Department of Energy, Office of High Energy Physics, under Contract No. DE-AC-02-05CH11231, and by the U.S. De-

partment of Energy SciDAC project, “Advanced Computing for 21st Century Accelerator Science and Technology,” which is supported by the Office of High Energy Physics and the Office of Advanced Scientific Computing Research.

APPENDIX: BEAM LOADING CONSIDERATIONS

Beam loading, whereby the trapped electron bunch significantly alters the accelerating wakefield, can degrade the quality of the electron bunch. Beam loading is neglected in the particle tracking code. To estimate the effects of beam loading, the wakefield generated by the trapped electron bunch propagating in an initially uniform plasma can be calculated and compared to the wakefield driven by the pump laser pulse. Using linear wakefield theory, the normalized density perturbation $\delta n/n_0 \ll 1$ and normalized axial electric field $E_z/E_0 \ll 1$ driven in an initially uniform plasma by a short electron bunch (n_b/n_0 drive term) is given by [16,17,21,22]

$$\left(\frac{\partial^2}{\partial \zeta^2} + k_p^2\right) \frac{\delta n}{n_0} = -k_p^2 \frac{n_b}{n_0}, \quad (\text{A1})$$

$$(\nabla_{\perp}^2 - k_p^2) \frac{E_z}{E_0} = -k_p \frac{\partial \delta n}{\partial \zeta n_0}, \quad (\text{A2})$$

where the drive bunch and the resulting wakefields are assumed to be functions of only the variables $\zeta = z - ct$ and r_{\perp} . Solving the system of equations (A1) and (A2) for a cylindrically symmetric drive n_b yields

$$\frac{\delta n}{n_0} = -k_p \int_{\infty}^{\zeta} d\zeta' \sin[k_p(\zeta - \zeta')] \frac{n_b(\zeta')}{n_0}, \quad (\text{A3})$$

$$\begin{aligned} \frac{E_z}{E_0} = & -k_p^3 \int_{\infty}^{\zeta} d\zeta' \int_0^{\infty} dr' r' \cos[k_p(\zeta - \zeta')] \\ & \times I_0(k_p r_{<}) K_0(k_p r_{>}) \frac{n_b(r', \zeta')}{n_0}, \end{aligned} \quad (\text{A4})$$

where I_0 and K_0 are the zeroth-order modified Bessel functions of the second kind and $r_{<}$ ($r_{>}$) denote the smaller (larger) of r and r' , respectively. For a uniform beam profile $n_b(r, \zeta) = n_b \Theta(r_b - r) \Theta(-\zeta) \Theta(\zeta + L)$ of radius r_b and length L , where Θ is a step function, the profile of the perturbed density and the axial wakefield are inside the bunch $-L \leq \zeta \leq 0$,

$$\delta n/n_0 = -2(n_b/n_0) \sin^2(k_p \zeta/2), \quad (\text{A5})$$

$$E_z/E_0 = -(n_b/n_0) F_R(r) \sin k_p \zeta, \quad (\text{A6})$$

and behind $\zeta < -L$,

$$\delta n/n_0 = 2(n_b/n_0) \sin(k_p L/2) \sin k_p(\zeta + L/2), \quad (\text{A7})$$

$$E_z/E_0 = -(n_b/n_0) F_R(r) [\sin k_p \zeta - \sin k_p(\zeta + L)], \quad (\text{A8})$$

where the radial profile function is

$$F_R(r) = \begin{cases} 1 - k_p r_b K_1(k_p r_b) I_0(k_p r), & \text{for } r < r_b, \\ k_p r_b I_1(k_p r_b) K_0(k_p r), & \text{for } r > r_b, \end{cases} \quad (\text{A9})$$

with I_1 and K_1 first-order modified Bessel functions. Assuming $k_p L \ll 1$ yields, at the back of the bunch,

$$\delta n/n_0 \approx -(k_p L)^2 (n_b/n_0)/2, \quad (\text{A10})$$

$$E_z/E_0 \approx k_p L (n_b/n_0) F_R(r). \quad (\text{A11})$$

-
- [1] E. Esarey, P. Sprangle, J. Krall, and A. Ting, *IEEE Trans. Plasma Sci.* **24**, 252 (1996).
- [2] K.-C. Tzeng, W. B. Mori, and T. Katsouleas, *Phys. Rev. Lett.* **79**, 5258 (1997).
- [3] E. Esarey, B. Hafizi, R. Hubbard, and A. Ting, *Phys. Rev. Lett.* **80**, 5552 (1998).
- [4] A. Pukhov and J. Meyer-ter-Vehn, *Appl. Phys. B: Lasers Opt.* **74**, 355 (2002).
- [5] F. S. Tsung, R. Narang, W. B. Mori, C. Joshi, R. A. Fonseca, and L. O. Silva, *Phys. Rev. Lett.* **93**, 185002 (2004).
- [6] S. V. Bulanov, F. Pegoraro, A. M. Pukhov, and A. S. Sakharov, *Phys. Rev. Lett.* **78**, 4205 (1997).
- [7] S. Bulanov, N. Naumova, F. Pegoraro, and J. Sakai, *Phys. Rev. E* **58**, R5257 (1998).
- [8] P. Tomassini, M. Galimberti, A. Giulietti, D. Giulietti, L. A. Gizzi, L. Labate, and F. Pegoraro, *Phys. Rev. ST Accel. Beams* **6**, 121301 (2003).
- [9] H. Suk, N. Barov, J. B. Rosenzweig, and E. Esarey, *Phys. Rev. Lett.* **86**, 1011 (2001).
- [10] C. Geddes, C. Toth, J. van Tilborg, E. Esarey, C. Schroeder, D. Bruhwiler, C. Nieter, J. Cary, and W. Leemans, *Nature (London)* **431**, 538 (2004).
- [11] D. Umstadter, J. K. Kim, and E. Dodd, *Phys. Rev. Lett.* **76**, 2073 (1996).
- [12] R. G. Hemker, K.-C. Tzeng, W. B. Mori, C. E. Clayton, and T. Katsouleas, *Phys. Rev. E* **57**, 5920 (1998).
- [13] J. R. Cary, R. E. Giaccone, C. Nieter, and D. L. Bruhwiler, *Phys. Plasmas* **12**, 056704 (2005).
- [14] E. Esarey, R. F. Hubbard, W. P. Leemans, A. Ting, and P. Sprangle, *Phys. Rev. Lett.* **79**, 2682 (1997).
- [15] C. B. Schroeder, P. B. Lee, J. S. Wurtele, E. Esarey, and W. P. Leemans, *Phys. Rev. E* **59**, 6037 (1999).
- [16] G. Fubiani, E. Esarey, C. B. Schroeder, and W. P. Leemans, *Phys. Rev. E* **70**, 016402 (2004).
- [17] G. Fubiani, Ph.D. thesis, Lawrence Berkeley National Laboratory and University Paris XI, Orsay, 2005.
- [18] H. Kotaki, S. Masuda, M. Kando, J. K. Koga, and K. Nakajima, *Phys. Plasmas* **11**, 3296 (2004).
- [19] E. Esarey, G. Fubiani, C. Schroeder, B. Shadwick, W. Leemans, J. Cary, and R. Giaccone, *Bull. Am. Phys. Soc.* **47**, 280 (2002).
- [20] E. Esarey and W. P. Leemans, *Phys. Rev. E* **59**, 1082 (1999).
- [21] R. Keinings and M. E. Jones, *Phys. Fluids* **30**, 252 (1987).
- [22] T. Katsouleas, S. Wilks, P. Chen, J. M. Dawson, and J. J. Su, *Part. Accel.* **22**, 81 (1987).